

When is a Stokes Line not a Stokes Line?

III Real Consequences of the Higher Order Stokes Phenomenon

C.J.Howls
University of Southampton

November 30, 2004

1 Introduction

From all the examples of the activity of Stokes lines in the previous two papers Howls (2005ab), the reader may be left with the impression that the higher order Stokes phenomenon is an analytical relic whose influence is confined to the complex plane. In this paper we demonstrate that this is far from true, and that the higher order Stokes phenomenon can result in far reaching effects in real space.

Here we shall study two pedagogical examples. The first is a linear partial differential equation similar to that of the second paper Howls (2005b). Here we shall show that the activity of Stokes lines has both a qualitative and quantitative effect on the large time behaviour of the solution. The second examples is Burgers equation. Although an integrable nonlinear PDE we study it because of its canonical role in the discussion of smoothed shock wave formation. We shall see that when viewed from an asymptotic problem, the higher order Stokes phenomenon is crucial to the mechanism for the formation of the shock.

2 Example: Linear Partial Differential Equation

We study the effect of the higher order Stokes phenomenon on the large time behaviour of the partial differential system $-\infty < x < +\infty, t > 0$,

$$u_t - u_x = \epsilon^2 u_{xxx} - \frac{1}{1+x^2}, \quad u(x, 0) = \arctan x, \quad (2.1)$$

where $u_x, u_{xx}, u_{xxx} \rightarrow 0$ as $|x| \rightarrow \infty$ and $0 < \epsilon \ll 1$. This system is intimately related to the PDE studied in the second paper above (Howls 2005b). The full details have also appeared in

Howls *et al* (2004). However here, for ease, we shall use an integral approach to illustrate the how the higher order Stokes phenomenon affects the remainder terms and expansions in different regions of the real $\mathbf{a} = (x, t)$ plane.

The system can be solved exactly by Fourier transforms as a sum of integrals

$$u(x, t; \epsilon) = \arctan x + \sum_{j=1}^2 I_j(x, t; \epsilon) + \sum_{j=3}^4 I_j(x; \epsilon), \quad (2.2)$$

where

$$I_1(x, t; \epsilon) = \int_0^{\infty} \frac{ip/2}{p^2 - 1} e^{-f(p; x, t)/\epsilon} dp = I_2^*(x, t; \epsilon), \quad (2.3)$$

$$I_3(x; \epsilon) = \int_0^{\infty} \frac{ip/2}{1 - p^2} e^{-p(1+ix)/\epsilon} dp = I_4^*(x; \epsilon), \quad (2.4)$$

and

$$f(p; x, t) = p(1 + ix) + ip(1 - p^2)t, \quad (2.5)$$

The star denotes complex conjugation. In I_1 and I_3 (respectively I_2 and I_4) the contours are indented around the poles at $p = +1$ in prescribed manner such that there is (initially) no overall pole contribution and the initial conditions are satisfied as $|x| \rightarrow \infty$

For $t > 0$, asymptotic contributions to I_1 and I_2 can arise from the endpoints at $p = 0$, the pole at $p = +1$, and one of two saddlepoints. For I_3 and I_4 , analogous contributions can only arise from the endpoint and the pole at $p = +1$.

To study the time evolution of the problem in the real (x, t) plane, without loss of generality we can restrict our attention to I_1 .

The endpoint at $p = 0$, is denoted by the superscript/subscripts e ; the pole at $+1$ by p_1 , at -1 by p_2 ; the saddles at

$$p = \pm \sqrt{\frac{1}{3it} (1 + i(x + t))} \quad (2.6)$$

by s_1 (for $+$) and s_2 (for $-$). The choice of notation is now seen to agree with the labelling of contributions in the second paper (Howls 2005b) allowing for the additional terms that arise from the sum of complex conjugates.

As we use the integral representations it is quite easy to see now that the asymptotic behaviours are given by:

$$e^{-f_j/\epsilon} T^{(j)}(\epsilon) \quad (2.7)$$

where j denotes e, s_1 or p_1 , with the following expressions

$$f_e(x, t) = 0, \quad T^{(e)}(\epsilon; x, t) \sim \frac{1}{2i} \sum_{r=1}^{\infty} \left(\sum_{m=0}^{r-1} \frac{\Gamma(2r+m)(it)^m}{m! (1+i(x+t))^{2r+m}} \right) \epsilon^{2r}, \quad (2.8)$$

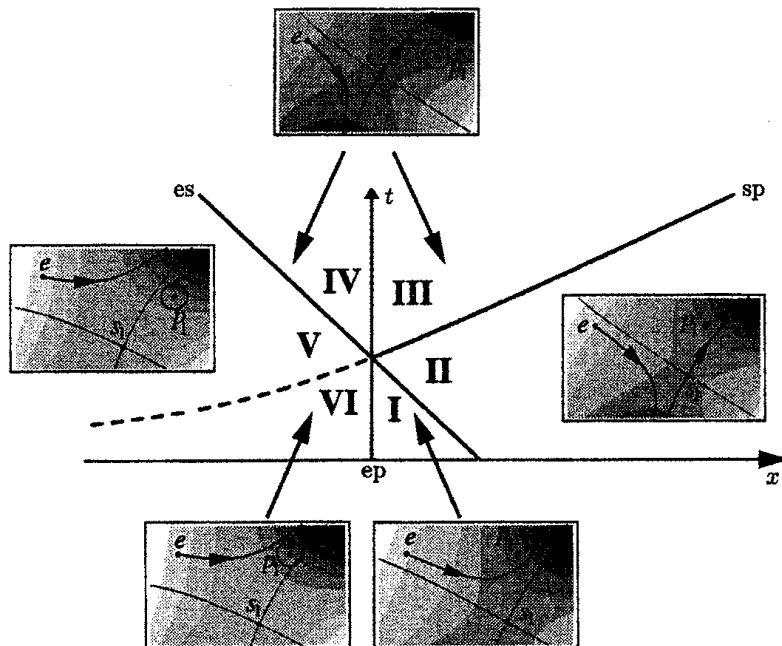


Figure 1: The six regions in the real $(x, t > 0)$ half-plane in which different asymptotic behaviours for I_1 are possible. These regions are delineated by Stokes lines. The notation “es”, for example, refers to an endpoint switching on a saddle contribution. The dashed Stokes line between V and VI is active, but irrelevant. The dotted line between regions III and IV is an inactive Stokes line.

$$f_{s_1}(x, t) = \frac{2i(x + t - i)^{3/2}}{3\sqrt{3t}}, \quad T^{(s_1)}(\epsilon; x, t) \sim \sum_{r=0}^{\infty} T_r^{(s_1)} \epsilon^{r+1/2}, \quad (2.9)$$

$$f_{p_1}(x, t) = 1 + ix, \quad T^{(p_1)}(\epsilon; x, t) = -\frac{1}{2}\pi. \quad (2.10)$$

The first coefficient of the saddlepoint expansion about s_1 is

$$T_0^{(s_1)} = \frac{1}{2}i\sqrt{\pi i} \frac{(3t)^{1/4} (x + t - i)^{1/4}}{x - 2t - i}. \quad (2.11)$$

It is important to note that contributions from the saddle and endpoint are both (asymptotic) infinite series. The single-term contribution from the pole is exact.

The conjugacy of I_2 and I_1 mean that they have analytically similar structures and the relevant expansions are just the corresponding conjugates of (4.8). The contributions from integral I_3 can be obtained by setting $t = 0$ in (2.9) and (2.10), and multiplying the results by -1 . The corresponding expansions for I_4 are the conjugates of those from I_3 .

With all the above contributions it is a straightforward task to draw the candidate Stokes curves in the real (x, t) plane, see figure 1.

There are three candidates for Stokes curves:

- the line $x = 0$ where

$$F_{ep_1}(x, t) \equiv f_{p_1} - f_e = 1 + ix > 0 \quad (2.12)$$

the endpoint may switch on a pole (residue) contribution;

- along a curve running forward in time from negative x to positive x where

$$F_{s_1p_1}(x, t) \equiv f_{p_1} - f_{s_1} = 1 + ix - 2i \frac{(x+t-i)^{3/2}}{3\sqrt{3t}} > 0 \quad (2.13)$$

a saddle may switch on a pole contribution;

- along the line $x + t = 1/\sqrt{3}$ running forward in time where

$$F_{es_1}(x, t) \equiv f_{s_1} - f_e = 2i \frac{(x+t-i)^{3/2}}{3\sqrt{3t}} > 0, \quad (2.14)$$

the endpoint may switch on a saddle.

An analysis of a sequence of plots of the steepest descent contours as a function of x and t leads to the findings of figure 2. The endpoint e contributes for all values of x and t .

In region **I**, only the endpoint term contributes. Across the Stokes line between regions **I** and **II**, the dominant endpoint switches on a subdominant contribution from s_1 . Across the Stokes curve between regions **II** and **III**, s_1 switches on a (relatively) subdominant contribution from p_1 (which in turn is sub-subdominant to the contribution from e). Crossing $x = 0$ from region **I** clockwise into region **VI**, e switches on a subdominant pole contribution from p_1 . This combination persists across the apparent Stokes line between s_1 , p_1 and into region **V**, since there is no s_1 yet present to switch on/off a contribution from p_1 . Across the line between **V** and **IV**, s_1 is finally switched on by e . Thus there are contributions from e , s_1 and p_1 in both regions **III** and **IV**.

From (2.12) the axis along $x = 0$, $t > 1/\sqrt{3}$ delineating regions **III** and **IV** should be a Stokes curve where a dominant e switches on or off a subdominant contribution from p_1 . However, the presence of such a Stokes curve would lead to a contradiction. For example, by continuing from region **III** anti-clockwise to **IV**, e should then switch off p_1 so that no contribution from p_1 existed in **IV**. To the contrary, the clockwise continuation around $t = 1/\sqrt{3}$ from region **I** suggests that **IV** should indeed contain a p_1 contribution. The conclusion is that despite the presence of the necessary dominant and subdominant terms, no Stokes phenomenon can take place. This is confirmed by a steepest descent analysis (see insets in figure 1).

This picture is entirely consistent with the Stokes curve geometry plotted for a real t -section in figure 4 of the second paper (Howls 2005b). When $t < 1/\sqrt{3}$, the kidney-shaped higher order

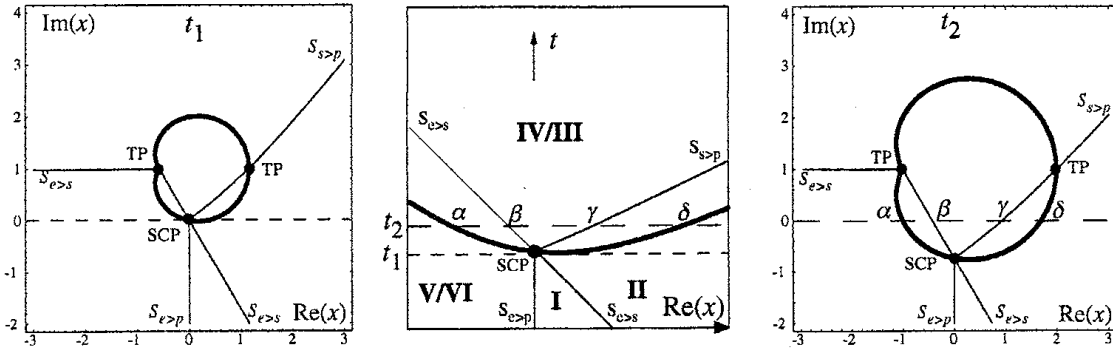


Figure 2: The Stokes curves (solid lines) and the higher order Stokes curve (bold line) for I_1 (centre pane) compared with real sections complex x -planes (left and right panes) at times $t = t_1 = 1/\sqrt{3}$ (dotted line in middle pane) and $t = t_2 > 1/\sqrt{3}$ (dashed line in middle pane). Only the active and relevant Stokes curves have been drawn. The kidney-shaped higher order Stokes curve grows in size from $t = 0^+$ and first intersects real (x, t) space at $t = t_1 = 1/\sqrt{3}$, the minimum of the higher order Stokes curve in real (x, t) space. Thereafter the Stokes curve S_{ep} is inactive. The points $\alpha, \beta, \gamma, \delta$ indicate the intersections of the Stokes and higher order Stokes curves at t_2 (right pane) with the real (x, t) plane (centre pane).

Stokes line in the complex x -plane does not intersect the real (x, t) plane. The Stokes curve $S_{e>p}$ is active for $\Im(x)$ below the SCP but inactive above the higher order Stokes curve. As t evolves between 0^+ and $1/\sqrt{3}$ the intersection of the active $S_{e>p}$ curve traces out the active Stokes line delineating regions **I** and **VI**. At $t = 1/\sqrt{3}$ the SCP intersects with real (x, t) plane at $(0, 1/\sqrt{3})$ and switches off the curve delineating regions **III** and **IV**. The curves delineating **II** and **III**, **IV** and **V** respectively, are still active. The locus of the points of intersection of the higher order Stokes curve in the complex x -plane and the real (x, t) plane is the U -shaped curve defined by

$$\frac{F_{es_1}}{F_{s_1p_1}} > 0, \quad (2.15)$$

that runs between infinities in regions **II** and **V**, through the point $(x, t) = (0, 1/\sqrt{3})$, see figure 2.

In figure 3 we display the overall combination of terms that contribute from the sum of the four integrals. For the integrals $I_3(x; \epsilon)$ and $I_4(x; \epsilon)$ a single Stokes line exists along the whole of the t -axis. Superposing this on the integrals $I_1(x, t; \epsilon)$ and $I_2(x, t; \epsilon)$ we find that the composite expansion has a Stokes line along the t -axis for $t > 1/\sqrt{3}$, but not for $t < 1/\sqrt{3}$. This does not alter the role of the higher order Stokes phenomenon, which has determined the constituent Stokes behaviour of $I_1(x, t; \epsilon)$ and $I_2(x, t; \epsilon)$. Hence, in regions **I**, **VI** and **V** only the endpoints of the four integrals contributes to the asymptotics. In region **II** and **IV**, there are also contributions from the saddle points, and region **III** is the only region where also the pole contributes.

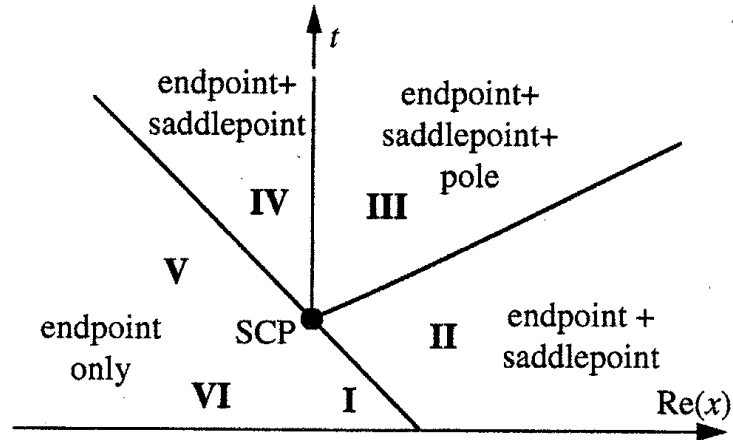


Figure 3: The active and relevant Stokes lines together with the asymptotic contributions in each region for the complete expansion of (2.1) generated by sum of integrals in (2.2).

A further significant consequence of this example is the necessity to include exponentially sub-subdominant terms in the large time asymptotic analysis. For $x > 0, t \approx 0$, the dominance of the asymptotic contributions is (cf. (2.12),(2.13),(2.14))

$$\left| e^{-f_e/\epsilon T(e)} \right| > \left| e^{-f_{s_1}/\epsilon T(s_1)} \right| > \left| e^{-f_{p_1}/\epsilon T(p_1)} \right|. \quad (2.16)$$

The longer time behaviour in region III involves all three such contributions, with $e^{-f_{s_1}/\epsilon T(s_1)}$ a decaying function of time but $e^{-f_{p_1}/\epsilon T(p_1)}$ independent of time. Consequently $e^{-f_{p_1}/\epsilon T(p_1)}$ develops as the principle time-independent oscillatory background to the monotonic $e^{-f_e/\epsilon T(e)}$. If the sub-subdominant $e^{-f_{p_1}/\epsilon T(p_1)}$ had been initially neglected as irrelevant near to $t = 0$, then an incorrect large- t , finite- x behaviour would have been predicted. This can be verified by carrying out a similar analysis for the other integrals I_2, I_3, I_4 and combining the results.

In figure 4 we display a comparison of a numerical evaluation of the sum of the four integrals in (2.2) in the real (x, t) -plane against the leading order behaviours of the asymptotics within each Stokes region for the $\epsilon = 0.125$. The plot in the middle of figure 4 is the sum of the four integrals, evaluated numerically. The brightness indicates the height. The plot at the bottom of figure 4 is the result of taking just the leading order behaviours of all asymptotic contributions in each region as detailed in figure 3.

In figure 5 we take a section for $t = 30, \epsilon = 0.5$ and plot the spatial dependence of solutions and approximations. The plot at the top is the leading order asymptotic approximation that started at $t = 0^+$ by ignoring the initially sub-subdominant $e^{-f_{p_1}/\epsilon T(p_1)}$. The middle plot is the exact solution. The bottom plot is the leading order asymptotic evolved according to the activity of Stokes lines.

The agreement within figures 4 and 5 is obvious in regions IV, V and VI when $x < 0$. The

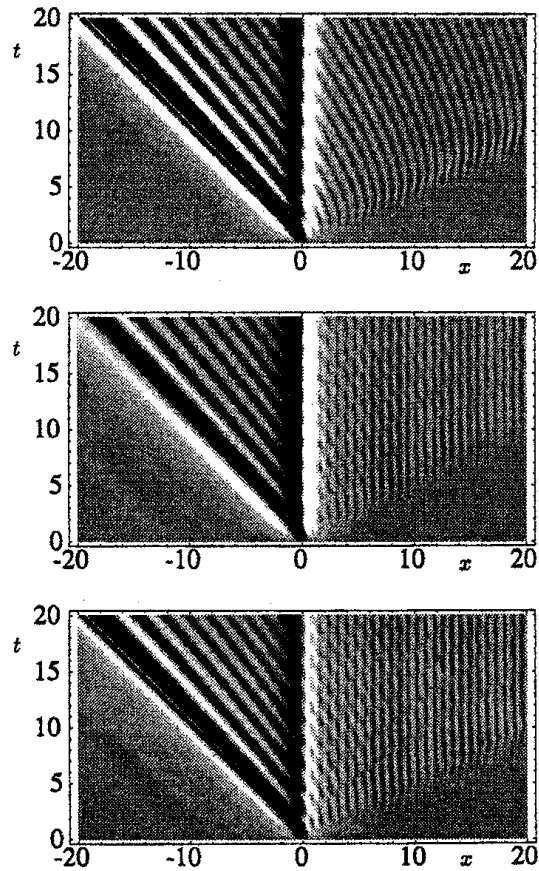


Figure 4: The plot in the middle is the solution of the PDE (2.1) minus $\arctan x$ with $\epsilon = 0.125$. The plot at the bottom is the result of taking leading order behaviours of all asymptotic contributions in each region (see figure 3), and the plot at the top is the same, except that the contributions from the sub-subdominant poles is omitted.

asymptotics arising from a neglect of the sub-subdominant pole (top plots) is however at odds with the exact result in region III. The exact wave structure is dominated at larger times in this region by the initially sub-subdominant pole contribution. A neglect of this would have resulted in a false conclusion being drawn as to the large-time behaviour. Finally only in the neighbourhoods of the active Stokes curves do we observe that the sum of the leading order behaviours changes discontinuously.

This example clearly demonstrates that the real time evolution of the solution of even linear PDEs may be affected by the change in activity of Stokes curves caused by higher order Stokes surfaces that emanate from complex singularities.

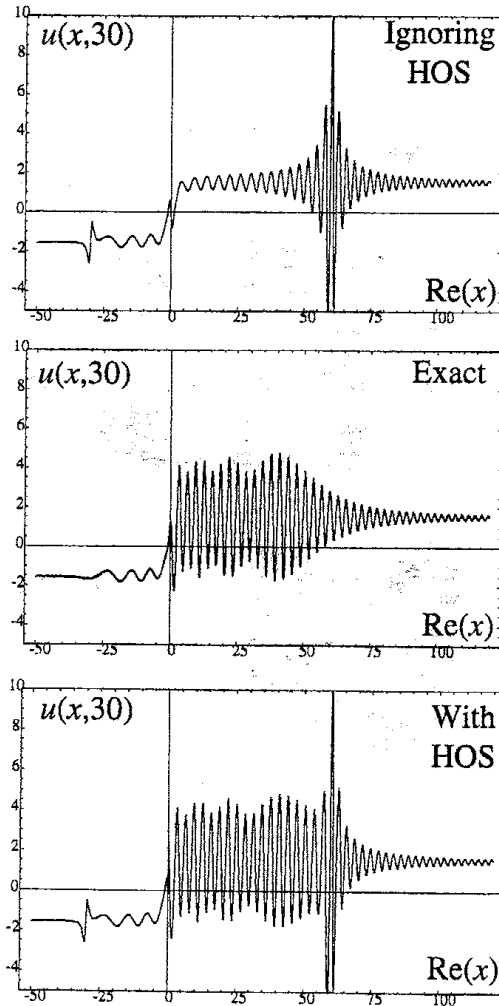


Figure 5: The plot in the middle is the exact solution of the PDE (2.1) at $t = 30$ obtained from quadrature with $\epsilon = 0.5$. The plot at the bottom is the result of taking leading order behaviours of all asymptotic contributions in each region and the plot at the top is the same, except that the contributions from the sub-subdominant poles is omitted. The disagreement between the exact and asymptotic approximations near to $t = -30$ and $t = 60$ is due to the proximity of the turning points TP in the complex plane at $x = 2t + i$ and $x = i - t$ which cause the leading orders to be the smallest term in the expansion, i.e., a non-uniform asymptotic analysis becomes questionable in this region.

3 Smoothed Shock Waves

In this example we demonstrate the effect of the higher order Stokes phenomenon on a nonlinear PDE in the real $\mathbf{a} = (x, t)$ plane. Specifically we will examine its role in the development of smoothed shock waves via the canonical example of Burgers equation. The extra asymptotic complications introduced into Borel-type analysis by nonlinearities are well discussed in the recent literature see for example (but not exclusively), Costin & Costin (2001), Costin & Kohut (2004), Costin & Tanveer (2004), Olde Daalhuis (2004ab).

We provide an overview of the work here, as the details will appear elsewhere Howls *et al* (2005).

We start with the Burgers equation

$$u_t + uu_x = \epsilon u_{xx}, \quad (3.1)$$

where

$$x \in \mathcal{C}, \quad t \geq 0, \quad \epsilon \rightarrow 0^+, \quad (3.2)$$

and choose initial Cauchy conditions

$$u(x, 0) = \frac{1}{1+x^2}, \quad \text{and } u \rightarrow 0 \text{ as } |x| \rightarrow \infty. \quad (3.3)$$

Obviously, Burgers equation may be solved using the Cole-Hopf integral representation, or using approximate matching techniques to locate the position of the smoothed shock that forms after a finite time. However we shall approach this pedagogical example from an exponential asymptotics point of view to provide an alternative, novel, view of the smoothed shock formation.

The small $\epsilon > 0$ expansion of the solution can be deduced to have a template of the form

$$u(x, t; \epsilon) \sim u^{(0)}(x, t; \epsilon) + \sum_{n=1}^{\infty} C_1^n u^{(n,1)}(x, t; \epsilon) + \sum_{n=1}^{\infty} C_2^n u^{(n,2)}(x, t; \epsilon) \quad (3.4)$$

where

$$u^{(0)}(x, t; \epsilon) \sim \sum_{r=0}^{\infty} a_r(x, t) \epsilon^r \quad (3.5)$$

$$u^{(n,j)}(x, t; \epsilon) \sim e^{-nf_j(x,t)/\epsilon} \sum_{r=0}^{\infty} a_r^{(n,j)}(x, t) \epsilon^r, \quad j = 1, 2, \quad n = 1, 2, 3, \dots \quad (3.6)$$

By substitution into (3.1) we see that $a_0(x, t)$ satisfies the inviscid Burgers equation

$$\frac{\partial a_0}{\partial t} + a_0 \frac{\partial a_0}{\partial x} = 0, \quad a_0(x, 0) = \frac{1}{1+x^2}, \quad (3.7)$$

and for $r \geq 1$ the $a_r(x, t)$ satisfy

$$\frac{\partial a_r}{\partial t} + \sum_{s=0}^r a_{r-s} \frac{\partial a_s}{\partial x} = \frac{\partial^2 a_{r-1}}{\partial x^2}, \quad a_r(x, 0) = 0. \quad (3.8)$$

The leading orders of the largest of the subdominant exponential contributions satisfy $\mathcal{O}(e^{-nf/\epsilon})$ generates

$$\frac{\partial a_0^{(1,j)}}{\partial t} + (a_0 + 2f_x) \frac{\partial a_0^{(1,j)}}{\partial x} + \left(\frac{\partial a_0}{\partial x} - a_1 f_x + f_{xx} \right) a_0^{(1,j)} = 0, \quad (3.9)$$

The exponential functions $f_j(x, t)$ satisfy the first order nonlinear equation

$$f_t + a_0 f_x + f_x^2 = 0. \quad (3.10)$$

The boundary data for these functions can be found by consideration of the rays of (3.7).

There are three rays of (3.7) through each point (x, t) . These are the lines

$$x = x_j + a_0(x_j)t, \quad j = 0, 1, 2, \quad (3.11)$$

where here and henceforth, we have abbreviated $a_0(x_j, 0)$ to $a_0(x_j)$ and the x_j are the intersection points of these rays with the complex plane $t = 0$, or alternatively, the locations of the saddlepoints in the Cole-Hopf solution. On these rays the a_0 take the constant values

$$a_0(x_j) = \frac{1}{1 + x_j^2}, \quad j = 0, 1, 2. \quad (3.12)$$

The root x_0 of (3.11) is chosen to be the one that is real for all real (x, t) . The families of rays generated by the x_j are tangential at caustics which simultaneously satisfy (3.11) and

$$0 = 1 + \frac{da_0(x_j)}{dx_j} t, \quad j = 0, 1, 2, \quad (3.13)$$

For the chosen initial conditions the caustics are given by

$$t = \frac{2}{27} \left(x(x^2 + 9) \pm (x^2 - 3)^{3/2} \right). \quad (3.14)$$

Since we restrict ourselves to $t > 0$ the caustics are one-dimensional curves. There are two real and two complex caustics in the (x, t) space under consideration, see figure 6. On the complex caustic with $\Im x > 0$, roots x_0 and x_1 coalesce and so we call this caustic \mathcal{C}_{01} . On the complex caustics with $\Im x < 0$, x_0 and x_2 coalesce and is thus labelled \mathcal{C}_{02} . On the real caustics \mathcal{C}_R , x_1 and x_2 coalesce.

These caustics \mathcal{C}_R separate the regions in the real (x, t) plane in which the classical smoothed shock of Burgers' equation forms ('inside' the caustic) from regions where the amplitude or the travelling wave changes over a longer spatial scale ('outside' the caustic), see figure 7.

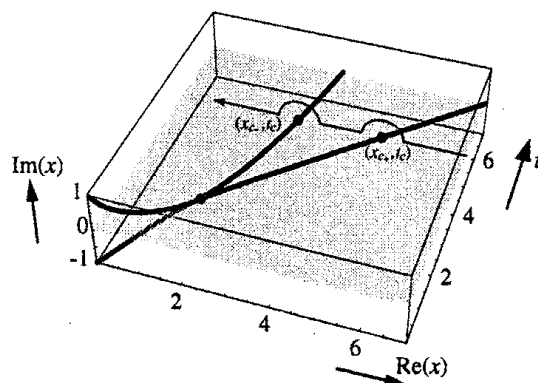


Figure 6: Caustics in complex x -space for real t and a path of analytic continuation around them.

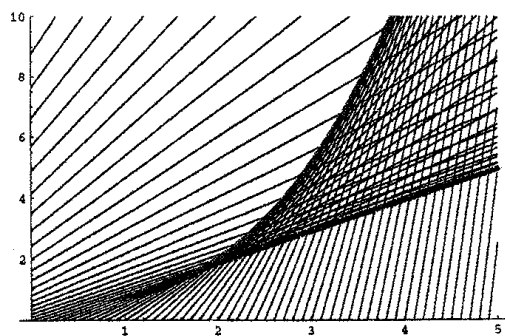


Figure 7: Rays and caustics for Burgers' equation with initial data (3.3) for $x, t \geq 0$. The real caustics are marked in bold.

As x_1 and x_2 are complex outside \mathcal{C}_R , imposition of reality on the solution is sufficient to ensure uniqueness of the solution in the real (x, t) plane outside the real caustics. The unique solution to the inviscid Burgers' equation outside the caustic in the real (x, t) plane is thus $a_0(x_0(x, t))$.

It is obvious, and well known, that inside \mathcal{C}_R , the multivalued leading order inviscid behaviour $a_0(x, t)$ that satisfies the inviscid Burgers' equation cannot adequately represent the solution of viscid Burgers' equation. By using exponential asymptotics the effect of the multivaluedness of $a_0(x, t)$ may be corrected.

Note that the a_0 appearing in (3.10) is identical to the choice of a_0 in the leading order behaviour u_0 in (3.5). It is therefore $a_0(x_0(x, t))$, which is completely determined by (3.7), where $x_0(x, t)$ is the real solution of (3.11).

The exponents $f_j(x, t)$ must vanish on the complex caustics, since here they coalesce with the exponent of the leading order solution, i.e., $f_0(x, t) \equiv 0$, so that the exponential correction terms are there of the same order as the first series in (3.4). Thus the boundary data for the solutions of (3.10) are

$$f_j(x, t) = 0 \quad \text{on } \mathcal{C}_{0j}, \quad j = 1, 2. \quad (3.15)$$

and

$$f_1(x, t) = f_2(x, t) \quad \text{on } \mathcal{C}_R. \quad (3.16)$$

Cole-Hopf, or direct analysis of the PDE reveals that

$$f_j(x(x_0, x_j), t(x_0, x_j)) = \frac{1}{2} \int_{x_0}^{x_j} a_0(z) dz - \frac{1}{4} (a_0(x_0) + a_0(x_j))(x_j - x_0), \quad (3.17)$$

$j = 1, 2$.

It can also be shown that

$$a_0^{(1,1)}(x_0, x_1) = (a_0(x_1) - a_0(x_0)) \sqrt{\frac{a_0(x_1) - a_0(x_0) - a_0'(x_0)(x_1 - x_0)}{a_0(x_1) - a_0(x_0) - a_0'(x_1)(x_1 - x_0)}}. \quad (3.18)$$

This results holds for all values of x_0 and x_1 .

We now turn to the singularity structure in the Borel plane. It is actually a lot more complicated than we shall outline here (see Howls *et al* 2005). However for the purposes of this paper it will suffice to consider the following simplified story.

The location of singularities visible from $\tau = f_0(x, t)$ are indicated in figure 8 for a typical value of (x, t) . From (3) we deduce that in the Borel plane, (logarithmic) branch-points exist at $\tau = n f_j$, $j = 1, 2$, $n = 1, 2, 3, \dots$. A detailed analysis of the transseries (see e.g., Olde Daalhuis 2004ab) or the Cole-Hopf representation shows that the Borel transform of $u^{(1,1)}(x, t; \tau)$ must see a branch-point at $\tau = f_2(x, t)$. Likewise the Borel transform of $u^{(1,2)}(x, t; \tau)$ must see a branch-point at $\tau = f_1(x, t)$.

Note that for certain values of (x, t) these singularities may appear to coalesce in the Borel plane. However only when the singularities lie on the same Riemann sheet can this give rise to actual caustics and divergences in the asymptotic representations.

Now we consider the analytic continuation of the transseries expansion in the real plane from regions outside the \mathcal{C}_R to inside. Without loss of generality, we perform this at a constant $t > 8/\sqrt{27}$. The space of continuation is therefore a complex x -plane in which the caustics degenerate to a pair of turning points. Due to symmetry of the initial conditions as $|x| \rightarrow \infty$ we shall also initially just consider the continuation around the turning point with the largest values of $\Re x$. We label this point x_{c+} .

We take a path in the complex x -plane along the points x_A, x_B, \dots , see figures 6, 8. This complex path is taken to avoid any singular behaviour in the exponentially small transseries $u^{(n,1)}$ and $u^{(n,2)}$, ($u^{(0)}$ is actually regular at \mathcal{C}_R), which nevertheless will play a vital role inside the caustic region. It is obviously possible to obtain a uniform asymptotic approximation across the caustic involving Airy functions. However we are interested here in the more fundamental exponential asymptotic behaviour that underpins other procedures.

Surrounding the central diagram of the complex x -plane in figure 8, are snapshots of the locations of the singularities as viewed from $\tau = f_0$ in the Borel plane at the positions x_A, x_B, \dots . As we move around the complex x -plane, the arrays of singularities will pivot about $f_0 = 0$.

We also plot the sections through the Stokes surfaces $S_{i>j}$ across which contributions involving f_i can switch on f_j . Note that at the turning point x_{c+} $f_1 = f_2 > 0$, hence this turning point does not directly involve f_0 . Thus the Stokes lines $S_{0>1}$ and $S_{0>2}$ both pass through the turning point inertly and f_0 dominates f_1 and f_2 all along this line in the vicinity of x_{c+} . On the other hand the Stokes lines $S_{1>2}$ and $S_{2>1}$ sprout at angles of $2\pi/3$ from x_{c+} (reflecting the Airy-type nature of the simple coalescence). A higher order curve S_{021} exists for (x, t) in the locality of x_{c+} and is also shown in figure 8. Note that a branch cut also emanates from $x > x_{c+}$. However, in what follows we can avoid all interaction with it, and so for simplicity we have not included it in the figure.

It transpires Howls *et al* (2005) that we only actually have to consider the Stokes lines $S_{0>1}$, $S_{0>2}$, $S_{1>2}$ and $S_{2>1}$.

We now start on the real x -axis outside the caustic region where $x > x_{c+}$. We pick a general point x_A , and aim to continue to $x < x_{c+}$ in the complex x -plane. At x_A , to satisfy the decay of u as $|x| \rightarrow \infty$ (3.3), comparison of the full template for the expansion (3) reveals that $C_1 = C_2 = 0$. Hence we have

$$u(x_A, t; \epsilon) \sim u^{(0)}(x_A, t; \epsilon), \quad (3.19)$$

as the complete asymptotic expansion.

At x_B we cross the Stokes line $S_{0>1}$. Here the array of singularities nf_1 , $n = 1, 2, 3, \dots$ lines

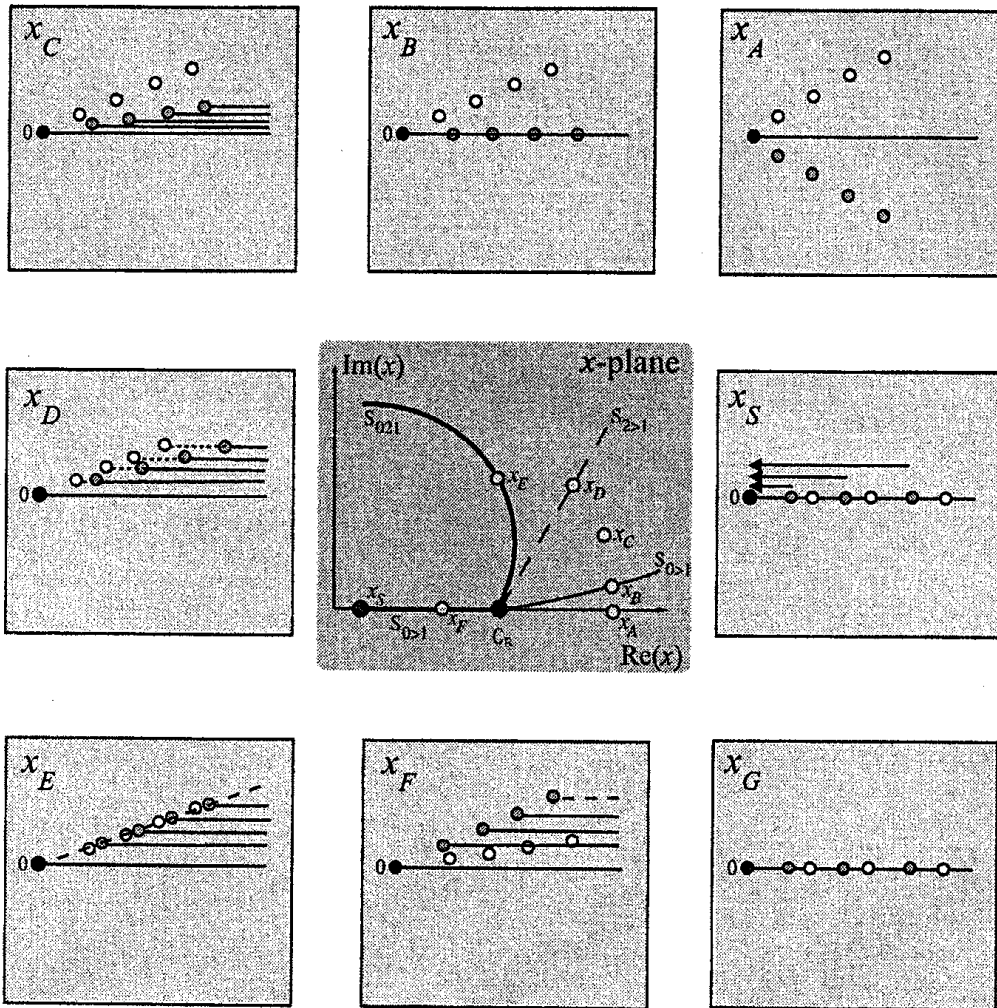


Figure 8: The central panel depicts part of the complex x -plane at constant $t > 8/\sqrt{27}$ for expansion (3.4) and illustrates the location of Stokes and higher order Stokes curves. Surrounding the central panel are snapshots of the distribution of singularities in the Borel plane, as seen from f_0 , at the various values of x indicated. See the main text for a full description of what happens at the indicated values of x .

up horizontally with the direction of Borel integration. Consequently a nonlinear Stokes phenomenon takes place involving all the nf_1 , see Olde Daalhuis (2004ab). After crossing the line (at point $x = x_C$) the asymptotics is now a transseries that takes the form

$$u(x, t; \epsilon) \sim u^{(0)}(x, t; \epsilon) + \sum_{n=1}^{\infty} K_{01}^n u^{(n,1)}(x, t; \epsilon), \quad (3.20)$$

where K_{01} is a Stokes constant. We can show (either from Cole-Hopf or directly from the PDE that $K_{01}=1$.

At x_D we encounter the Stokes line $S_{2>1}$. At this point singularity $f_1 - f_2 > 0$ and so there is a potential for a Stokes phenomenon to take place. However, singularity f_2 is not contributing to the transseries expansion of the function we are interested in at x_D . Hence no Stokes phenomenon between f_2 and f_1 actually takes place and this is again an irrelevant Stokes curve.

At x_E , we encounter the higher order Stokes line S_{021} . On this curve the Borel singularities f_0 , f_1 and f_2 and all their multiples are collinear. Here we see that rather than having a finite number of collinear singularities, we must deal with an infinite set, leading to an infinite number of Riemann sheets.

As in linear cases, since $|f_1| > |f_2|$, on the line of collinearity in the Borel plane the singularity f_2 lies in between f_0 and f_1 . When we cross the higher order Stokes line, when viewed from f_0 , the singularity at f_1 moves across a cut from f_2 and onto a different Riemann sheet from f_0 .

A more detailed analysis of all the other singularities Howls *et al* (2005) shows that on crossing the higher order Stokes line all the singularities in the array $f_1, 2f_1, 3f_1, \dots$ move on to mutually different Riemann sheets and are so are directly invisible from the original expansion point f_0 , and the singularities nf_1 can no longer see mf_1 , $m \neq n$.

At x_F , the arrays are no-longer collinear with one another. However the nf_1 are still collinear with f_0 : just because they might be on different Riemann sheets, this does not grant them the autonomy to move independently.

At x_G , where x is real, but $x < x_{c+}$, f_0 and the arrays nf_1, mf_2 are all again colinear, this time along the horizontal direction of Borel integration and $0 < f_1 < f_2$. A Stokes line therefore potentially exists between f_0 and the nf_1 . However, since the nf_1 are now all on different Riemann sheets from f_0 , they are invisible to f_0 and cannot cross the actual Borel integration contour, which is anchored at f_0 but on the principal Riemann sheets. Thus the the Stokes line $S_{0>1}$ is inactive and no Stokes phenomenon between f_0 and any element of nf_1 takes place. There is also the possibility of a Stokes phenomenon between f_0 and nf_2 or even f_1 and nf_2 , but these are of lower exponential order and will not concern us here.

It is important now to recall that $x = x_{c+}$ is not a turning point/caustic for 0 and nf_1 . Hence the activity of the the Stokes curve $0 > 1$ has changed at a regular point across the higher order

Stokes curve that passes through $x = x_{c+}$.

We now examine the structure of the ‘dominant’ part of the transseries on the real x -axis inside \mathcal{C}_R

$$u(x, t; \epsilon) = a_0(x, t) + \sum_{n=1}^{\infty} K_{01}^n e^{-nf_1(x,t)/\epsilon} a_0^{(n,1)}(x, t) + \mathcal{O}(\epsilon), \quad (3.21)$$

as $\epsilon \rightarrow 0+$. Exponentially small terms are included before the $\mathcal{O}(\epsilon)$ in (3.21) because we are now in a region where $f_1(x, t)$ may decrease to zero. There is thus the possibility that these exponentially small terms can interfere with the $\mathcal{O}(1)$ terms.

We combine (3.5), (3.6) and (3.10) and are able to deduce for $n = 2, 3, 4, \dots$, that

$$a_0^{(n,1)} = \left(a_0^{(1,1)}\right)^n \left(-2 \frac{\partial f_1}{\partial x}\right)^{1-n}. \quad (3.22)$$

This simple relationship allows us to sum the n -sum in the transseries (3.21) and obtain

$$u(x, t; \epsilon) = a_0(x, t) + \frac{2K_{01}a_0^{(1,1)}(x, t)\frac{\partial f_1}{\partial x}e^{-f_1/\epsilon}}{2\frac{\partial f_1}{\partial x} + K_{01}a_0^{(1,1)}(x, t)e^{-f_1/\epsilon}} + \mathcal{O}(\epsilon), \quad (3.23)$$

as $\epsilon \rightarrow 0+$. This result is valid everywhere in the region where $\Re f_1 > 0$ and may be analytically continued to the region where $\Re f_1 \leq 0$.

If we continue along the line $S_{0>1}$, in the negative x -direction the singularities nf_1 all move towards f_0 in the Borel plane, see x_H . At the point (x_S, t) the nf_1 appear to coalesce with f_0 . This is the point at which an exchange of dominance in the asymptotic expansion takes place. Classically, this is the position of the smoothed shock, where the solution changes abruptly from one value to the next.

Due to the coalescence of the exponents, from a naive point of view, this point is apparently a caustic/turning point of the asymptotics. If this were a true turning point the derivatives in individual terms in the asymptotics would diverge at x_S . An examination of the coefficients $a_r(x, t)$ (Howls *et al* 2005) shows that this is not the case. The reason for this is that, as suggested above, all the singularities nf_1 and 0 *indeed do lie on mutually different Riemann sheets*: this is only an apparent coalescence. This is a virtual turning point.

We may now conclude with the following key observations (further discussion may be found in Howls *al* 2005).

The terms themselves in the transseries do not diverge at the position of the smoothed shock x_S . This is because x_S is only a virtual turning point, since all the Borel singularities are on mutually different Riemann sheets. Hence the Borel singularities have accumulated to create a smooth shock rather than a caustic.

The reason that the Borel singularities are on mutually different sheets is the presence of the higher order Stokes curve. Without the higher order Stokes curve the Riemann sheet structure of the Borel plane would not change and the coalescence of Borel singularities at the shock point would have resulted in divergence of individual terms in the asymptotics. Put simply, if it were not for the higher order Stokes phenomenon, the shock would be a caustic. In fact the position of the shock is a moving virtual caustic (or virtual turning point).

Hence, when viewed from the standpoint of exponential asymptotics, the higher order Stokes phenomenon is an essential part of the mechanism for forming the smoothed (propagating) shock.

The resummed transeries solution (3.23) is valid for values of $x < x_S$. It is thus a way of continuing the solution through the nonlinear anti-Stokes line that passes locally vertically through the virtual turning point.

Although this is only one specific smoothed shock problem, we believe the mechanism explained above is more general. Clearly a smoothed shock is a change of dominance between contributions in an expansion. If these take the form of exponentially prefactored series, then a Borel plane structure similar to that described above will exist. If the boundary data is such that (infinitely) many singularities are contributing to the asymptotics near to the smoothed shock, and if the asymptotics does not diverge at that shock, then the Borel singularities must lie on mutually different sheets. This may well have arisen because of the crossing of a higher order Stokes curve.

4 Conclusion

In this paper we have concluded the discussion of the higher order Stokes phenomenon by showing its relevance to the large time asymptotics of linear PDE problems and smoothed shock formation in a nonlinear PDE.

The relevance of the higher order Stokes phenomenon to a problem will be determined both by the problem and the boundary data associated with it. The difficulty in practically examining its effects in ODEs or PDEs should not be underestimated. Nevertheless in canonical problems, some progress can be made and extra insight can be obtained into the underlying analytic structure of the asymptotics.

Acknowledgements

This work was supported by EPSRC grant GR/R18642/01 and by a travel grant from the Research Institute for Mathematical Sciences, University of Kyoto.

References

Costin, O. , Costin R.D., 2001, *On the formation of singularities of solutions of nonlinear differential systems in antistokes directions*, *Inventiones Mathematicae* 145, 3, pp 425-485.

Costin, O. , Costin R. D., Kohut M., 2004, *Rigorous bounds of Stokes constants for some nonlinear ODEs at rank one irregular singularities* *Proc. Roy. Soc. Lond.. In Press*

Costin, O, Tanveer , S. , 2004, *Nonlinear evolution of PDEs in $\mathbb{R}^+ \times C^d$: existence and uniqueness of solutions, asymptotic and Borel summability*, preprint Rutgers University.

Howls, C. J., Langman P., Olde Daalhuis A. B. , 2004, *On the higher order Stokes phenomenon* *Proc. R. Soc. Lond. A* **460**, 2585-2303.

Howls, C.J. ,2005a, *When is a Stokes line not a Stokes line? I. The higher order Stokes phenomenon*, this volume.

Howls, C.J. , 2005b, *When is a Stokes line not a Stokes line? II. Examples involving differential equations*, this volume.

Howls C.J., Olde Daalhuis A.B., 2005, *When is a shock not a caustic?* In preparation.

Olde Daalhuis, A. B., 2004a, *Hyperasymptotics for nonlinear ODEs I: A Riccati equation*, submitted to *R. Soc. Lond. Proc. Ser. A Math. Phys. Eng. Sci.*

Olde Daalhuis, A. B., 2004b, *Hyperasymptotics for nonlinear ODEs II: The first Painlevé equation and a second order Riccati equation*, submitted to *R. Soc. Lond. Proc. Ser. A Math. Phys. Eng. Sci.*